



# Assessing the Heterogeneity of Response of [<sup>68</sup>Ga] Ga-PSMA-11 PET/CT Lesions in Patients With Biochemical Recurrence of Prostate Cancer

Mikaela Dell'Oro,<sup>1</sup> Daniel T. Huff,<sup>2</sup> Ojaswita Lokre,<sup>2</sup> Jake Kendrick,<sup>3,4</sup> Rajkumar Munian Govindan,<sup>2</sup> Jeremy S.L. Ong,<sup>5</sup> Martin A. Ebert,<sup>1,3,4,6</sup> Timothy G. Perk,<sup>2</sup> Roslyn J. Francis<sup>1,7</sup>

## Abstract

**In this study, special imaging called PSMA PET/CT was analyzed for 199 men with advanced prostate cancer. Computer software was used to monitor each tumor over 6-months. The research found that 25% of men had tumors that responded differently, which was linked to shorter overall survival. Recognizing these patients early could help doctors monitor them closely and provide treatment sooner.**

**Introduction:** Treatment of men with metastatic prostate cancer can be difficult due to the heterogeneity of response of lesions. [<sup>68</sup>Ga]Ga-PSMA-11 (PSMA) PET/CT assists with monitoring and directing clinical intervention; however, the impact of response heterogeneity has yet to be related to outcome measures. The aim of this study was to assess the impact of quantitative imaging information on the value of PSMA PET/CT to assess patient outcomes in response evaluation. **Patients and Methods:** Baseline and follow-up (6 months) PSMA PET/CT of 162 men with oligometastatic PC treated with standard clinical care were acquired between 2015 and 2016 for analysis. An augmentative software medical device was used to track lesions between scans and quantify lesion change to categorize them as either new, increasing, stable, decreasing, or disappeared. Quantitative imaging features describing the size, intensity, extent, change, and heterogeneity of change (based on percent change in SUV<sub>total</sub>) among lesions were extracted and evaluated for association with overall survival (OS) using Cox regression models. Model performance was evaluated using the c-index. **Results:** Forty-one (25%) of subjects demonstrated heterogeneous response at follow-up, defined as having at least 1 new or increasing lesion and at least 1 decreasing or disappeared lesion. Subjects with heterogeneous response demonstrated significantly shorter OS than subjects without (median OS = 76.6 months vs. median OS not reached,  $P < .05$ , c-index = 0.61). In univariate analyses, SUV<sub>total</sub> at follow-up was most strongly associated with OS (HR = 1.29 [1.19, 1.40],  $P < .001$ , c-index = 0.73). Multivariable models applied using heterogeneity of change features demonstrated higher performance (c-index = 0.79) than models without (c-index = 0.71-0.76,  $P < .05$ ). **Conclusion:** Augmentative software tools enhance the evaluation change on serial PSMA PET scans and can facilitate lesional evaluation between timepoints. This study demonstrates that a heterogeneous response at a lesional level may impact adversely on patient outcomes and supports further investigation to evaluate the role of imaging to guide individualized patient management to improve clinical outcomes.

*Clinical Genitourinary Cancer*, Vol. 22, No. 5, 102155 © 2024 The Author(s). Published by Elsevier Inc. This is an open access article under the CC BY license (<http://creativecommons.org/licenses/by/4.0/>)

**Keywords:** Metastatic prostate cancer, PSMA PET/CT, Image features, Response heterogeneity

<sup>1</sup>Australian Centre for Quantitative Imaging, School of Medicine, The University of Western Australia, Perth, Australia

<sup>2</sup>AIQ Solutions, Madison, WI

<sup>3</sup>School of Physics, Mathematics and Computing, The University of Western Australia, Perth, Australia

<sup>4</sup>Centre for Advanced Technologies in Cancer Research, Perth, Australia

<sup>5</sup>Department of Nuclear Medicine, Fiona Stanley Hospital, Murdoch, Australia

<sup>6</sup>Department of Radiation Oncology, Sir Charles Gairdner Hospital, Nedlands, Australia

<sup>7</sup>Department of Nuclear Medicine, Sir Charles Gairdner Hospital, Nedlands, Australia

Submitted: Mar 26, 2024; Revised: Jul 2, 2024; Accepted: Jul 3, 2024; Epub: 6 July 2024

1558-7673/\$ - see front matter © 2024 The Author(s). Published by Elsevier Inc. This is an open access article under the CC BY license (<http://creativecommons.org/licenses/by/4.0/>) <https://doi.org/10.1016/j.clgc.2024.102155>

## Introduction

Prostate cancer is the most common cancer affecting men in Australia,<sup>1</sup> and throughout the world.<sup>2</sup> Over one third of men experience biochemical recurrence following primary curative

Address for correspondence: Mikaela Dell'Oro, PhD, Australian Centre for Quantitative Imaging, School of Medicine, The University of Western Australia, Level 5, Harry Perkins, 5 Verdun St, Perth, WA, 6009, Australia  
E-mail contact: [mikaela.delloro@uwa.edu.au](mailto:mikaela.delloro@uwa.edu.au)

## Assessing the Heterogeneity of Response

therapy, and this is associated with worse patient outcomes.<sup>3</sup> For subjects with biochemically recurrent prostate cancer (BCR PCa), measuring changes in tumor burden over time is crucial to evaluate treatment response and guide therapy selection. However, patient response is often complex and heterogeneous. In cases where a heterogeneous response is present, it is often difficult to assess whether a patient is benefiting from the current treatment regimen and how to proceed with subsequent treatment.<sup>4</sup>

Prostate-specific membrane antigen (PSMA) is a membrane-bound protein overexpressed on the surface of prostate cancer cells.<sup>5</sup> Positron emission tomography/computed tomography (PET/CT) utilizing PSMA radiolabelled with <sup>68</sup>Gallium (<sup>68</sup>Ga]Ga-PSMA-11) is an emerging modality for the management of subjects with BCR PCa.<sup>6,7</sup> Multiple sets of standardized PSMA PET-based response criteria have been proposed and evaluated.<sup>8-12</sup> However, the optimal utilization of the quantitative information provided by PSMA PET/CT for BCR PCa patient management has yet to be determined. Considering the rapidly evolving landscape of targeted treatments for BCR PCa actionable and early response assessment is needed.

Enabling the assessment of every lesion has clinical value because the extent and number of lesions not responding to treatment has been shown to be associated with outcomes in BCR PCa,<sup>4,13,14</sup> and the size, margins, and locations of lesions may influence treatment decisions. Automated software devices can alleviate the time burden by quantifying the size, extent, intensity, and distribution of all lesions, and by tracking individual lesions in time, allowing for automated quantification and assessment of heterogeneity of change in response to treatment. Capturing the overall disease burden permits the assessment of response criteria based on all lesions or a subset (1-5 lesions), providing a more comprehensive evaluation, and leading to better prediction of patient outcomes.

The goal of this study was to use an augmentative software medical device to analyse heterogeneity of response of lesions in PSMA PET/CT images of men with BCR PCa, and to assess the impact of changes in various quantitative imaging features on the performance of models of patient outcome. We hypothesized that the inclusion of quantitative imaging features that capture longitudinal change in disease and lesion-specific heterogeneity of change would improve model performance.

## Patients and Methods

### Study Population

The study performs a retrospective analysis using data collected as part of previous work<sup>15</sup> under clinical studies approved by the Human Research Ethics Committees of Sir Charles Gairdner Hospital (RGS1736), Fiona Stanley Hospital (2015-125) and The University of Western Australia (2019/RA/4/20/6382). Data for this study was collected based on the inclusion criteria of a previous prospective study evaluating change in management for patients which were negative or oligometastatic (maximum of 3 lesions) on bone scintigraphy and abdominal CT staging scans. Eligible participants had a baseline <sup>68</sup>Ga]Ga-PSMA-11 PET/CT scan at BCR and follow up <sup>68</sup>Ga]Ga-PSMA-11 PET/CT scan on 6 month follow up. Biochemical recurrence was defined as either: (i) prostate-specific antigen (PSA) levels greater than 0.2 ng/mL measured at least 6

weeks post radical prostatectomy, or (ii) PSA level at least 2 ng/mL above the previous PSA nadir measured at least 3 months post external beam radiotherapy.

A total of 398 <sup>68</sup>Ga]Ga-PSMA-11 PET/CT scans from 162 subjects with BCR PCa were acquired between 2015 and 2016 and were available for analysis. Between the baseline and follow up <sup>68</sup>Ga]Ga-PSMA-11 PET/CT scan subjects underwent therapy according to standard clinical care, which included radiotherapy to the prostatic bed, regional nodes or bone metastases, further surgery, systemic treatment in the form of chemotherapy or androgen deprivation therapy (ADT), or active surveillance.

### PET/CT Acquisition

The <sup>68</sup>Ga]Ga-PSMA-11 PET/CT scans were obtained from a Siemens Biograph 64, Biograph 128 or Biograph mCT 64 PET/CT scanner (CTI Inc, Knoxville TN) at either Sir Charles Gairdner Hospital or Fiona Stanley Hospital. Two MBq/kg of <sup>68</sup>Ga]Ga-PSMA-11 was administered intravenously through a peripheral intravenous cannula as a slow push. PET/CT image acquisition began approximately 1 hour after radiotracer administration. Prior to acquisition, subjects were asked to void their bladders. First, the low-dose CT (50 mAs, 120 kVp) was acquired from the middle of the thigh to the vertex of the skull for attenuation correction. Emission data were acquired immediately following the CT acquisition to ensure identical field of view. CT data were reconstructed to voxel resolutions between  $0.98 \times 0.98 \times 2 \text{ mm}^3$  and  $1.52 \times 1.52 \times 5 \text{ mm}^3$ . PET data were reconstructed to a voxel resolution of  $4.07 \times 4.07 \times 2 \text{ mm}^3$ .

### Image Analysis

PET images were normalized by subject body weight and injected activity to calculate Standardized Uptake Values (SUV). PSMA-positive lesions were identified and manually delineated by a Nuclear Medicine physician (author J.O.) with 5 years' experience with PSMA PET/CT using *MIM Encore* (MIM Software Inc., Cleveland, OH, USA).

PET/CT images were deidentified and prepared for local cloud-based analysis. Images were analyzed using *TRAQinform IQ* software (AIQ Solutions, Madison, WI, USA) to automatically quantify physician-delineated lesion regions of interest (ROI) on the baseline and follow-up scans, and to track and quantify changes in individual ROI between scans. *TRAQinform IQ* is a software medical device that performs comprehensive ROI-level estimation of anatomical and functional change derived from augmentative software analysis of multiple CT or PET/CT scans including total and individual changes of tracer uptake, radiodensity volumes, and heterogeneity of change, with interpretation and report then performed by a physician or other qualified healthcare professional using the output of the software medical device.

From each PET/CT image, 5 single-timepoint image features were extracted:  $SUV_{max}$ , defined as the maximum SUV within any ROI;  $SUV_{mean}$ , defined as the mean of SUV across all ROI; volume, defined as the volume of all ROI;  $SUV_{total}$ , defined as the product of  $SUV_{mean}$  and volume; and ROI count, defined as the number of lesions identified. Image features were extracted from both the baseline and follow-up scans. Percent change in each feature was

**Table 1** Published Literature Indicates That 30% Changes in  $SUV_{total}$  Can be Used to Determine Meaningful Changes in Lesions Over Time.<sup>18,17</sup> ROI Response Categories. Change in ROI  $SUV_{total}$  is Defined as  $\Delta SUV_{total} = 100\% \times (SUV_{total, F} - SUV_{total, B}) / SUV_{total, B}$ .

| Category    | Criteria                                  |
|-------------|---|
| New         | ROI not detected on baseline PET/CT       |
| Increasing  | $\Delta SUV_{total} > 30\%$               |
| Stable      | $-30\% \leq \Delta SUV_{total} \leq 30\%$ |
| Decreasing  | $\Delta SUV_{total} < -30\%$              |
| Disappeared | ROI not detected on follow-up PET/CT      |

also calculated as:  $100\% \times (SUV_F - SUV_B) / SUV_B$ , where  $SUV_B$  and  $SUV_F$  are the feature values for that subject on the baseline and follow-up scans, respectively.

Individual ROI were tracked between baseline and follow-up scans and classified as new, increasing, stable, decreasing, or disappeared based on their percent change in  $SUV_{total}$  (Table 1), enabling the extraction of image features quantifying lesion heterogeneity of change. The following heterogeneity features were extracted for each subject: the number of ROI in each category (e.g., the number of new ROI, the number of increasing ROI), the proportion of ROI in each category (e.g., the proportion of ROI classified as new), and the  $SUV_{max}$ ,  $SUV_{mean}$ ,  $SUV_{total}$ , and volume of ROI in each category (e.g., the  $SUV_{max}$  of increasing ROI).

Subjects were assigned to 1 of 3 categories depending on the presence of ROI by response category:

- Homogeneous response: subjects with only disappeared, decreasing, or stable ROI.
- Homogeneous progression: subjects with only new, increasing, or stable ROI, or with exclusively stable ROI.
- Heterogeneous response: subjects who had at least 1 disappeared or decreasing ROI and at least 1 new or increasing ROI.

### Survival Models

Quantitative imaging features were assessed for their potential to stratify subjects by overall survival (OS) using Cox proportional hazards regressions. A complete listing of individual quantitative imaging features within each feature set used for univariate and multivariable analysis are detailed in Table 2. As previously described, OS was defined as the time between the follow-up PSMA PET/CT and death following previous work.<sup>14</sup> In the case of surviving subjects, OS data were censored to the amount of time between the follow-up PSMA PET/CT and the censor date (March 13, 2023).

**Varied Input Feature Sets.** To evaluate the importance of different image features, multivariable Cox models were trained using multiple feature sets. Feature sets were assessed cumulatively, where each feature set includes features from the previous sets (e.g., baseline only, baseline plus follow-up, baseline plus follow-up plus longitudinal change, etc). For each feature set, 1000 bootstrap samples were constructed and the c-index for that sample to order subjects correctly by OS was calculated. The 4 feature sets were:

- (1) Baseline only: single-timepoint image features extracted from baseline images only.
- (2) +Follow-up: the previous feature set, plus single-timepoint image features extracted from the follow-up images only.
- (3) +Longitudinal change: the previous feature set, plus the percent change in each single-timepoint feature from baseline to follow-up.
- (4) +Heterogeneity: the previous feature set, plus the lesion heterogeneity of change features.

**Varied Number of Target Lesions.** To evaluate the importance of analyzing all lesions in a subject, 5 models were fit using different sets of target lesions selected on each scan. Target lesion sets were designed to capture either the largest ROI by volume, or the most metabolically active ROI, as characterized by  $SUV_{max}$ . Sets of 1 and up to 5 ROI were used, to match other published response criteria.<sup>18,19</sup> For this experiment, the +Heterogeneity feature set was used for all models. As in the analysis of varied input feature sets, 1000 bootstrap samples were constructed and the c-index was calculated. The 5 target lesion sets were:

- (1) One hottest: where the single ROI with highest  $SUV_{max}$  is considered,
- (2) One largest: where the single ROI with the highest volume is considered,
- (3) Five hottest: where up to the 5 ROI with the highest  $SUV_{max}$  are considered,
- (4) Five largest: where up to the 5 ROI with the highest volume are considered,
- (5) All: where all ROI are considered.

### Statistical Analysis

Continuous variables are reported as median (range), and categorical variables are reported as number and percentage. The association between PSMA PET/CT image features and OS was assessed using Cox proportional hazards regressions. The Box-Cox transform was used to ensure normality of image feature values.<sup>20</sup> The hazard ratio (HR), its 95% confidence interval (95%CI), and associated *P*-value were derived. The performance of fitted models was quantified using Harrell's concordance-index (c-index). Statistical analyses were carried out using Python's lifelines (version 0.27.8)<sup>21</sup> package and R (version 4.3.2).<sup>22</sup>

## Results

### Subject Characteristics

Subject characteristics are summarized in Table 3. A total of 398 [<sup>68</sup>Ga]Ga-PSMA-11 PET/CT images from 199 men with BCR PCa were initially identified. Of these, 37/199 (19%) had no disease identified on PET/CT at both imaging timepoints and were excluded, leaving 162 subjects for analysis.

For the included subjects, the median age was 70 years (range 46-90). The median time between baseline and follow-up PSMA PET/CT was 6.0 months (range: 3.2-8.5), and the median OS was 79.1 months (range: 6.1-87.6). Total 49/162 (30%) subjects experienced an event prior to the censor date.

# Assessing the Heterogeneity of Response

**Table 2** PSMA PET/CT Image Features by Feature Set.

| Feature                | Description   | Feature Set |             |                       |                 |
|------------------------|---|-------------|-------------|-----------------------|-----------------|
|                        |   | Baseline    | + Follow-Up | + Longitudinal Change | + Heterogeneity |
| Global max 1           | SUV <sub>max</sub> on the baseline scan.  | x           | x           | x                     | x               |
| Global mean 1          | SUV <sub>mean</sub> on the baseline scan.   | x           | x           | x                     | x               |
| Global volume 1        | Volume on the baseline scan.  | x           | x           | x                     | x               |
| Global total 1         | SUV <sub>total</sub> on the baseline scan.  | x           | x           | x                     | x               |
| Global count 1         | The number of ROI on the baseline scan.   | x           | x           | x                     | x               |
| Global max 2           | SUV <sub>max</sub> on the follow-up scan.   |             | x           | x                     | x               |
| Global mean 2          | SUV <sub>mean</sub> on the follow-up scan.  |             | x           | x                     | x               |
| Global volume 2        | Volume on the follow-up scan.   |             | x           | x                     | x               |
| Global total 2         | SUV <sub>total</sub> on the follow-up scan.   |             | x           | x                     | x               |
| Global count 2         | The number of ROI on the follow-up scan.  |             | x           | x                     | x               |
| Global max response    | Change in SUV <sub>max</sub> from baseline to follow-up.                                      |             |             | x                     | x               |
| Global mean response   | Change in SUV <sub>mean</sub> from baseline to follow-up.                                     |             |             | x                     | x               |
| Global volume response | Change in Volume from baseline to follow-up.  |             |             | x                     | x               |
| Global total response  | Change in SUV <sub>total</sub> from baseline to follow-up.                                    |             |             | x                     | x               |
| Global count response  | Change in the number of ROI from baseline to follow-up.                                       |             |             | x                     | x               |
| nDIS                   | The number of disappeared ROI at follow-up.   |             |             |                       | x               |
| nDEC                   | The number of decreasing ROI at follow-up.  |             |             |                       | x               |
| nSTB                   | The number of stable ROI at follow-up.  |             |             |                       | x               |
| nINC                   | The number of increasing ROI at follow-up.  |             |             |                       | x               |
| nNEW                   | The number of new ROI at follow-up.   |             |             |                       | x               |
| pctDIS                 | The percentage of disappeared ROI at follow-up.   |             |             |                       | x               |
| pctDEC                 | The percentage of decreasing ROI at follow-up.  |             |             |                       | x               |
| pctSTB                 | The percentage of stable ROI at follow-up.  |             |             |                       | x               |
| pctINC                 | The percentage of increasing ROI at follow-up.  |             |             |                       | x               |
| pctNEW                 | The percentage of new ROI at follow-up.   |             |             |                       | x               |
| Heterogeneous response | A binary feature: True if at least 1 DIS or DEC ROI and at least 1 INC or NEW ROI is present. |             |             |                       | x               |
| Inc. max 1             | SUV <sub>max</sub> at baseline of ROI that increase.  |             |             |                       | x               |
| Inc. mean 1            | SUV <sub>mean</sub> at baseline of ROI that increase.   |             |             |                       | x               |
| Inc. total 1           | SUV <sub>total</sub> at baseline of ROI that increase.  |             |             |                       | x               |
| Inc. count 1           | The number of ROI at baseline that increase.  |             |             |                       | x               |
| Inc. max 2             | SUV <sub>max</sub> at follow-up of ROI that increase.   |             |             |                       | x               |
| Inc. mean 2            | SUV <sub>mean</sub> at follow-up of ROI that increase.  |             |             |                       | x               |
| Inc. total 2           | SUV <sub>total</sub> at follow-up of ROI that increase.                                       |             |             |                       | x               |
| Inc. count 2           | The number of ROI at follow-up that increase.   |             |             |                       | x               |
| Inc. max response      | Change in SUV <sub>max</sub> from baseline to follow-up of ROI that increase.                 |             |             |                       | x               |
| Inc. mean response     | Change in SUV <sub>mean</sub> from baseline to follow-up of ROI that increase.                |             |             |                       | x               |
| Inc. total response    | Change in SUV <sub>total</sub> from baseline to follow-up of ROI that increase.               |             |             |                       | x               |
| Dec. max 1             | SUV <sub>max</sub> at baseline of ROI that decrease.  |             |             |                       | x               |
| Dec. mean 1            | SUV <sub>mean</sub> at baseline of ROI that decrease.   |             |             |                       | x               |
| Dec. total 1           | SUV <sub>total</sub> at baseline of ROI that decrease.  |             |             |                       | x               |
| Dec. count 1           | The number of ROI at baseline that decrease.  |             |             |                       | x               |
| Dec. max 2             | SUV <sub>max</sub> at follow-up of ROI that decrease.   |             |             |                       | x               |
| Dec. mean 2            | SUV <sub>mean</sub> at follow-up of ROI that decrease.  |             |             |                       | x               |

(continued on next page)

**Table 2** (continued)

| Feature             | Description   | Feature Set |             |                       |                 |
|---------------------|---|-------------|-------------|-----------------------|-----------------|
|                     |   | Baseline    | + Follow-Up | + Longitudinal Change | + Heterogeneity |
| Dec. total 2        | SUV <sub>total</sub> at follow-up of ROI that decrease.                         |             |             |                       | X               |
| Dec. count 2        | The number of ROI at follow-up that decrease.                                   |             |             |                       | X               |
| Dec. max response   | Change in SUV <sub>max</sub> from baseline to follow-up of ROI that decrease.   |             |             |                       | X               |
| Dec. mean response  | Change in SUV <sub>mean</sub> from baseline to follow-up of ROI that decrease.  |             |             |                       | X               |
| Dec. total response | Change in SUV <sub>total</sub> from baseline to follow-up of ROI that decrease. |             |             |                       | X               |

**Table 3** Subject Characteristics. Subjects May Have Received 1 or More Treatment Between Scans, Thus the Percentages for Treatment Between Scans Sum to Greater Than 100%. Gleason Score Data was Not Available for 4 Subjects.

| Characteristic                         | Number           | %   |
|--|------------------|-----|
| Subjects                               | 162              | 100 |
| Age [y]                                | -                | -   |
| Median (range)                         | 70 (46-90)       | -   |
| PSA at baseline PSMA PET scan [ng/mL]  | -                | -   |
| Median (range)                         | 3.7 (0.2-79.46)  | -   |
| PSA at follow up PSMA PET scan [ng/mL] | -                | -   |
| Median (range)                         | 3.3 (0.01-120.8) | -   |
| Gleason score                          | -                | -   |
| < 8                                    | 86               | 54  |
| ≥ 8                                    | 72               | 46  |
| Treatment between scans                | -                | -   |
| Radiotherapy                           | 58               | 36  |
| Surgery                                | 6                | 4   |
| Chemotherapy                           | 9                | 6   |
| Androgen-deprivation                   | 102              | 63  |
| Surveillance                           | 15               | 9   |
| Unknown                                | 17               | 10  |
| Time to follow-up PET [mo]             | -                | -   |
| Median (range)                         | 6.0 (3.2-8.5)    | -   |
| OS [mo]                                | -                | -   |
| Median (range)                         | 79.1 (6.1-87.6)  | -   |

### Disease Burden on PSMA PET/CT

Physician review of the PSMA PET/CT images identified 607 lesions at baseline (median 1 per subject, range 0-33), and 628 at follow-up (median 1 per subject, range 0-100). The median disease volume was 3.2 mL (range 0-112.3) at baseline and 2.3 mL (range 0-507.9) at follow-up.

### Lesion Response Heterogeneity

In the final cohort, 41/162 (25%) subjects demonstrated heterogeneous response. Of patients without heterogeneous response, 71/162 (44%) demonstrated homogeneous response, and 50/162 (31%) demonstrated homogeneous progression. Lesion-wise hetero-

geneity of change is summarized in Figure 1. Volume renderings of selected subjects demonstrating each response categorization are shown in Figure 2.

Subjects classified as having heterogeneous response demonstrated significantly shorter OS compared to subjects with homogeneous response (log-rank test,  $P < .001$ ), and compared to subjects with homogeneous progression (log-rank test,  $P = .04$ ). Kaplan-Meier curves with subjects stratified by response category are shown in Figure 3.

### Univariate Survival Models

The prognostic value of individual quantitative imaging features was evaluated using univariate Cox proportional hazards regressions (Figure 4). The PSMA imaging feature which demonstrated the strongest association with OS was SUV<sub>total</sub> on the follow-up scan (c-index = 0.728, HR = 1.29 [1.19-1.40],  $P < .001$ ). Similar performance was seen for SUV<sub>max</sub> on the follow-up scan (c-index = 0.725), and disease volume on the follow-up scan (c-index = 0.704). Disease burden metrics at baseline were also associated with OS ( $P < .05$ ) including disease volume at baseline (c-index = 0.685), SUV<sub>total</sub> at baseline (c-index = 0.681), and number of lesions at baseline (c-index = 0.654). Kaplan-Meier curves of the highest performing feature in each category are shown in Figure 5.

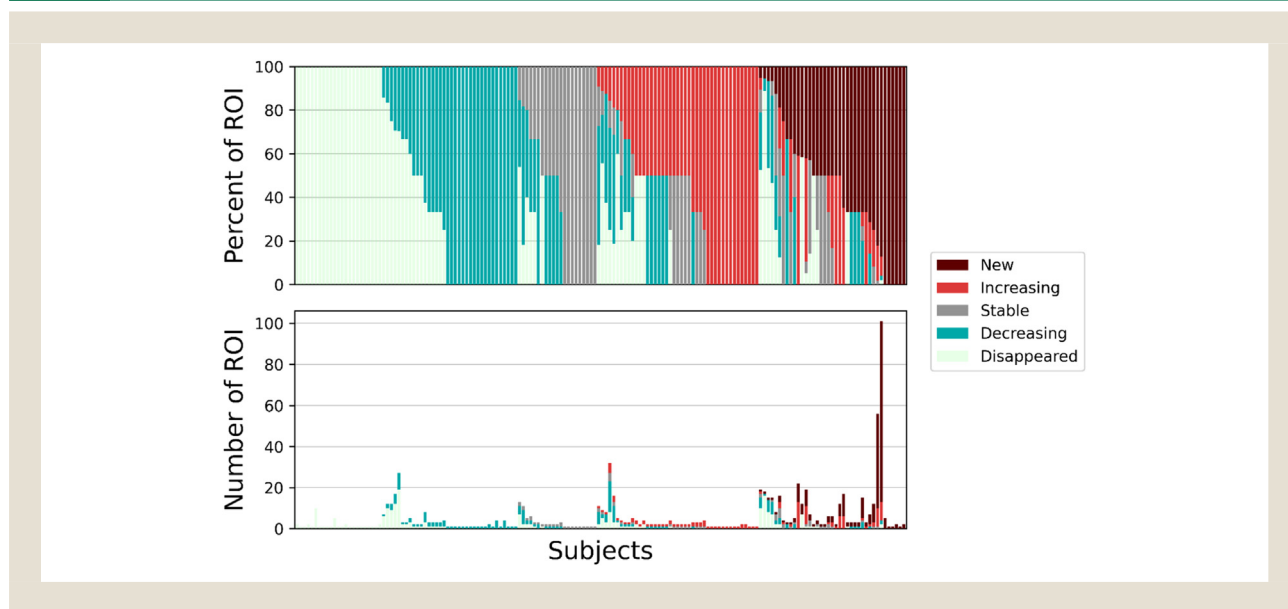
Of features characterizing lesion heterogeneity of change, features describing the number, extent, and intensity of lesions which increased in PSMA SUV<sub>total</sub> were more strongly associated with OS than features describing lesions which decreased in PSMA SUV<sub>total</sub>. For example, the SUV<sub>max</sub> of increasing lesions (c-index = 0.670) outperformed the SUV<sub>max</sub> of decreasing lesions (c-index = 0.580). In general, lesion count features were outperformed by other features, with the number of stable ROI (c-index = 0.619) and the number of new ROI (c-index = 0.613) achieving the highest performance.

### Multivariable Survival Models

**Varied Input Feature Sets.** For the 4 feature sets, the c-indices across bootstrap samples were (mean ± sd): baseline only 0.716 ± 0.036, +follow-up 0.765 ± 0.030, +longitudinal change 0.777 ± 0.031, and +heterogeneity 0.795 ± 0.029. Adding each successive feature group resulted in a significant increase in c-index (2-sample t-test,  $P < .05$ , Bonferroni corrected for 3 comparisons).

## Assessing the Heterogeneity of Response

**Figure 1** Lesion-wise heterogeneity of change in 162 BCR PCa patient imaged with [<sup>68</sup>Ga]Ga-PSMA-11 PET/CT. Each column represents 1 subject, where the column is divided into colors representing the percent (top) or number (bottom) of ROI in each response category.



Box plots summarizing performance of models fit on each feature set are shown in Figure 6A.

**Varied number of Target Lesions.** The *c*-indices for the 5 ROI sets were (mean  $\pm$  sd): 1 hottest  $0.757 \pm 0.031$ , 1 largest  $0.789 \pm 0.028$ , 5 hottest  $0.795 \pm 0.030$ , 5 largest  $0.792 \pm 0.032$ , and all  $0.795 \pm 0.029$ . The model fit using the 1 hottest lesion was outperformed by all other lesion sets. Additionally, the model fit using the 1 largest lesion was outperformed by models fit using the 5 hottest and all lesion sets. Box plots summarizing performance of models fit on each lesion set are shown in Figure 6B.

## Discussion

In this study, PSMA PET/CT images of 162 men with BCR PCa were analyzed using an augmentative software medical device which enabled lesion tracking over time to calculate longitudinal change in disease from baseline (acquired prior to treatment) to follow-up (after 6 months on therapy). In this cohort, 25% of men demonstrated heterogeneous response, where 1 or more lesion disappeared or was associated with decreasing PSMA uptake, and there were additional lesions that were new or were associated with increasing PSMA uptake. Subjects with heterogeneous response as assessed by PSMA PET/CT demonstrated significantly shorter OS than subjects with homogeneous response (median OS = 76.6 months vs. median OS not reached,  $P < .001$ ), as well as subjects with homogeneous progression (median OS = 76.6 months vs. median OS not reached,  $P = .04$ ). Identifying this subset of oligometastatic patients with heterogeneous response is important as it was found to be associated with reduced OS in this study, suggesting there may be an opportunity to intervene in this patient group to improve outcomes.

To assess the impact of quantifying lesion heterogeneity of change on the prognostic value of PSMA PET/CT, we fit multivariable Cox regression models on varied sets of image features extracted from the PET images. PSMA PET/CT scans capture heterogeneity across disease sites, providing insight into disease biology in addition to evaluating tumor burden. These insights can complement PSA measurements and potentially lead to more optimal treatment strategies. The inclusion of image features characterizing lesion heterogeneity of change increased model performance, demonstrating the value of software medical device assessment of lesion heterogeneity of change for potential to contribute to therapeutic decision-making in this cohort of oligometastatic BCR PCa patients imaged with PSMA PET/CT.

In univariate analysis, the feature most strongly associated with OS was  $SUV_{total}$  on the follow-up PSMA PET/CT (*c*-index = 0.73). Heterogeneity features capturing the extent and intensity of lesions increasing in PSMA activity at follow-up were more strongly associated with OS (*c*-index = 0.64-0.67) than features capturing lesions decreasing in total PSMA activity (*c*-index = 0.52-0.59), suggesting the critical role that disease increasing in size or PSMA expression has in driving disease progression and patient outcome.  $SUV_{total}$  at the 6 month follow-up was more strongly associated with patient outcome than the same metric at baseline (*c*-index = 0.73 vs. *c*-index = 0.68), suggesting the added value of follow-up PSMA PET/CT in the setting of treatment response assessment.

To assess the impact of performing comprehensive response assessment of all lesions versus sampling only a subset of ROI, as is undertaken in commonly used response criteria such as RECIST<sup>18</sup> or PERCIST,<sup>19</sup> multivariable Cox regression models using lesion quantification features extracted from different sets of target lesions were applied. When only 1 lesion with the highest  $SUV_{max}$  or only 1 lesion with the highest volume was quantified, model

**Figure 2** Volume renderings of selected example subjects. Subject skeletons and select organs are rendered in grey, and overlaid with disease ROI colored by response category, as determined by Table 1. Homogeneous response: a 76-year-old man receiving ADT treatment imaged with PSMA PET/CT at month 6 demonstrates homogeneous response, with 2 lesions in the pubis and proximal femur decreasing in  $SUV_{total}$ . This subject was still alive at time of censoring 86 months after follow-up imaging. Homogeneous progression: a 73-year-old man receiving ADT treatment imaged with PSMA PET/CT at month 6 demonstrates homogeneous progression, with numerous new PSMA-avid lesions appearing throughout the axial skeleton. Existing lesions in the pubis and lumbar spine demonstrate increased PSMA  $SUV_{total}$ . The overall survival for this subject was 62 months after follow-up imaging. Heterogeneous response: an 83-year-old man receiving ADT treatment imaged with PSMA PET/CT at month 8 demonstrates heterogeneous response, with several sites of nodal disease in the abdomen decreasing in  $SUV_{total}$  while several others are increasing, and 1 thoracic lesion demonstrating stable PSMA uptake. The overall survival for this subject was 30 months after follow-up imaging.

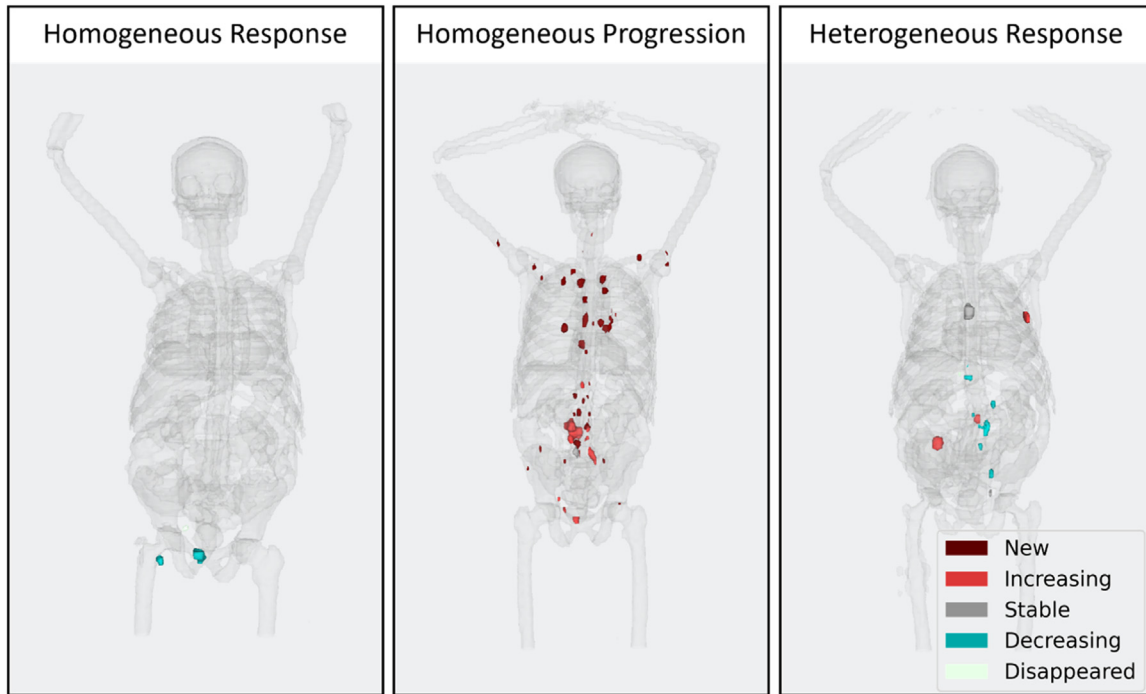
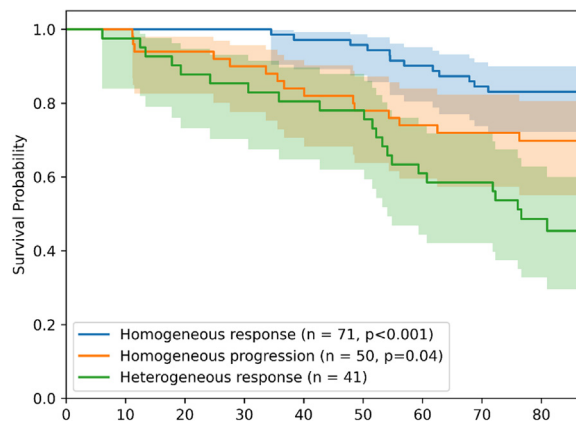
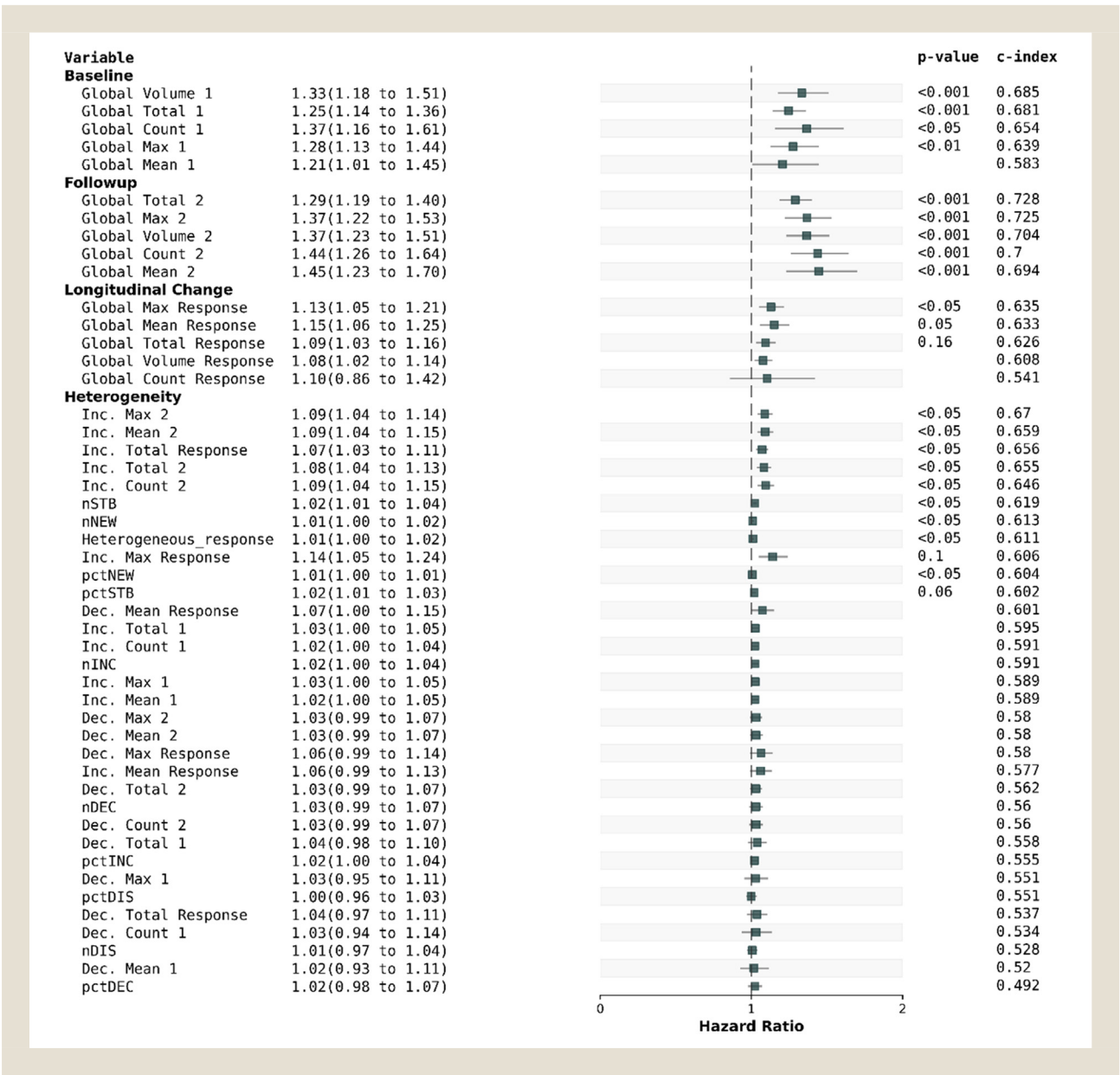


**Figure 3** Kaplan–Meier curve of subject OS by response group. Subjects with exclusively stable, decreasing, or disappeared lesions were classified as homogeneous response. Subjects with exclusively stable, increasing, or new lesions were classified as homogeneous progression. All other subjects were classified as heterogeneous response. The  $P$ -values compare OS between each homogeneous group and the heterogeneous response group (log-rank test).



# Assessing the Heterogeneity of Response

**Figure 4** Forest plot of univariate predictors. Features are divided by category and sorted by c-index within each category. Log-rank test was used to test each feature for association with OS. *P*-values are Bonferroni corrected for multiple hypotheses (*n* = 48), and *P* > .2 are not reported. Inc. = Increasing, Dec. = Decreasing. NEW = new lesions, INC = increasing lesions, STB = stable lesions, DEC = decreasing lesions, DIS = disappeared lesions. See Table 1 for definitions of lesion response categories.



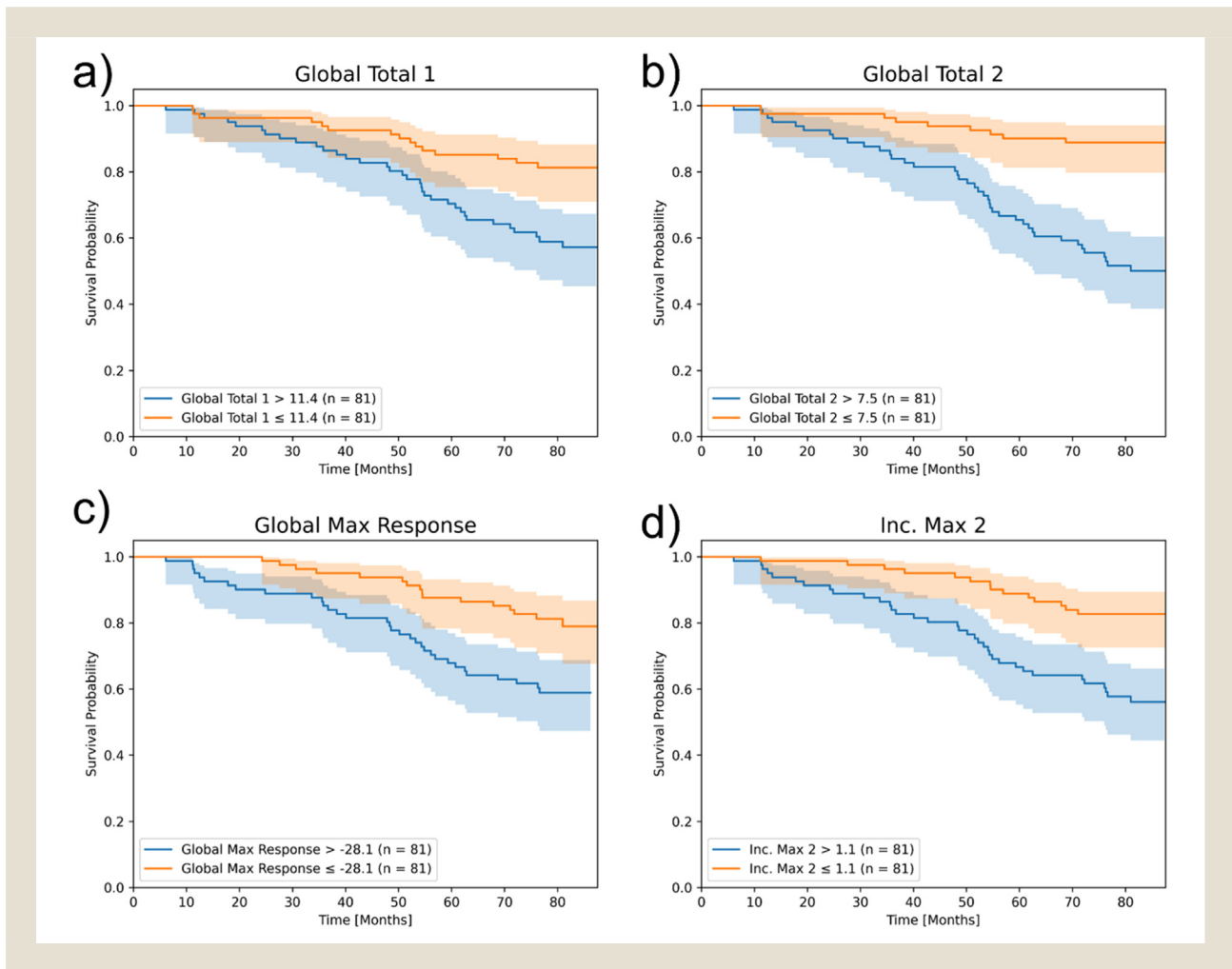
performance was significantly diminished relative to quantifying all lesions. When 5 lesions with the highest  $SUV_{max}$  or highest volume were quantified, no difference in model performance was observed relative to quantification of all lesions. This may be explained by the relatively low disease burden in the study cohort, where 121/162 (75%) of subjects had fewer than 5 lesions, meaning that using a RECIST-like sampling of up to 5 target lesions would result in quantification of all lesions present. This characteristic of the study cohort can be explained by the study inclusion criteria,<sup>14</sup> which required participants to demonstrate either no evidence of disease,

or only oligometastatic disease (<3 lesions) on bone scan or CT imaging. We hypothesize that if a similar analysis were conducted in a cohort of subjects with higher disease burden, a difference in the prognostic value of quantifying all lesions may be observed.

In this study cohort, subjects with heterogeneous response demonstrated shorter OS than subjects with either homogeneous response or homogeneous progression. While the appearance of new lesions, or increase in PSMA-avid disease volume on PSMA PET/CT has been demonstrated to be associated with worse outcomes,<sup>23</sup> the prognostic significance of heterogeneous response



**Figure 5** Kaplan–Meier curves for the highest performing feature in each feature category: (A) Baseline: Global Total 1: the overall burden SUV<sub>total</sub> of disease at baseline. (B) Follow-up: Global Total 2: the overall burden SUV<sub>total</sub> of disease at follow-up. (C) Longitudinal change: Global Max Response: the percent change in SUV<sub>max</sub> from baseline to follow-up. (D) Heterogeneity: Inc. Max. 2: the SUV<sub>max</sub> of increasing lesions at follow-up.

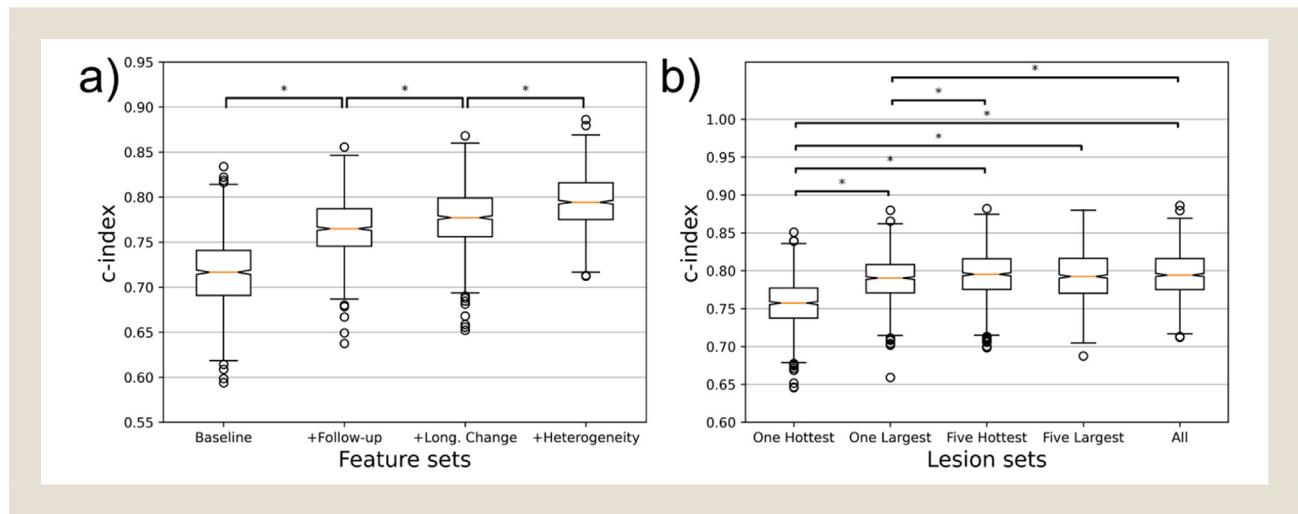


is unclear, and the finding that subjects with heterogeneous response demonstrate shorter OS than subjects with homogeneous progression is perhaps unexpected. It is possible that a response categorization of heterogeneous response reflects adverse genomic or biological heterogeneity of disease, and even if some lesions do respond to the current treatment, future treatments may be ineffective, leading to shorter OS. This finding may also be attributable to the varied treatment schedules received by subjects in the study cohort, as subjects with homogeneous progression at the time of follow-up imaging may have then changed treatment, leading to improved outcome. Conversely, subjects with heterogeneous response at follow-up may have remained on a treatment that only a subset of their disease was responding to, leading to poorer outcome. Future work in prospectively collected cohorts is required to determine the clinical implications of homogeneous versus heterogeneous response.

Previous work by our group has investigated the prognostic value of PSMA PET/CT in this cohort of patients.<sup>14</sup> The current study

adds to our previous work in several important areas, including the use of an augmentative software medical device to perform lesion matching, the assessment of image features that characterize lesion heterogeneity of change, and the assessment of varied image feature sets and target lesion sets on the prognostic value of PSMA PET/CT in BCR PCa. Other groups have also conducted similar studies in similar patient cohorts. In a retrospective analysis of 58 men with BCR PCa, Harsini et al. found that the number of lesions detected on PSMA PET/CT was associated with biochemical progression-free survival.<sup>24</sup> This is in line with our analysis, where the number of lesions at both baseline (c-index = 0.65) and follow-up (c-index = 0.70) were associated with OS. In a similar analysis of PSMA PET images of 103 men receiving <sup>177</sup>Lu-PSMA radioligand therapy (RLT), lower SUV<sub>mean</sub> at baseline was associated with reduced OS.<sup>25</sup> In our analysis baseline SUV<sub>mean</sub> was not associated with patient OS (c-index = 0.58). This may be attributed to the different in treatments between cohorts. Subjects in<sup>25</sup> received

**Figure 6** Performance of multivariable Cox models fit on varied Feature Sets (A) and Lesion sets (B) to order BCR PCa subjects by OS. Feature sets were assessed cumulatively, where each feature set includes the features from the previous sets. For “Largest” lesion sets, lesions were sorted by volume with the top N (e.g.,  $n = 1$ ,  $n = 5$ ) lesions being retained for quantification. For “Hottest” lesion sets, lesions were sorted by  $SUV_{max}$  with the top N lesions being retained for quantification. For “All”, all lesions were retained for quantification. Boxes summaries 1000 bootstrapped samples. Asterisks indicate significant differences between distributions (2-sample t-test,  $P < .05$ , Bonferroni corrected).



$^{177}\text{Lu}$ -PSMA RLT, whereas subjects in our cohort received a mix of surgery, chemotherapy, external beam radiotherapy, and hormonal therapy.

Software devices and the functions they perform for the clinician such as the device utilized in this study may provide value in any setting where the assessment of lesion-specific response is desired. For example, Probst et al. assessed interval changes in PSMA PET/CT before and after 6 cycles of  $^{223}\text{Ra}$  RLT.<sup>26</sup> The authors note that 89% of patients had PSMA PET progressive disease, however all patients also demonstrated decreases in PSMA uptake in some disease sites. Automated quantification of lesion-specific changes in PSMA uptake may provide value in this context. This description of discordant changes matches the definition of heterogeneous response used in our study, where patients have both newly appearing or increasing lesions and disappearing or decreasing lesions. Heterogeneous response, also called dissociated response, is an emerging pattern of response shown to occur in 8%-48% of patients depending on disease, stage, and treatment modality.<sup>27</sup> In our study, heterogeneous response was associated with reduced OS, however literature assessing whether this pattern of response is a positive or negative prognostic factor are mixed,<sup>28-31</sup> perhaps due to variations in the methods used to define this pattern of response. The prognostic implications of heterogeneous response are likely to depend on disease, stage, treatment, and other factors.

In our study, all disease ROI were delineated by a nuclear medicine physician. While this is feasible in a research setting, manual delineation of all disease ROI in a clinical setting is laborious and not routinely undertaken with clinical workflows due to the high time requirement. Automated delineation of whole-body PET/CT via deep learning has been demonstrated to be feasible both by our group,<sup>32</sup> and by others.<sup>33-35</sup> However, these tools are not yet available in routine clinical practice.

This study had several limitations which should be discussed. Subjects in the study cohort were imaged with PSMA PET/CT while receiving a variety of localized and systemic treatments including external beam radiotherapy, further surgery, chemotherapy, androgen deprivation therapy, and active surveillance. The burden of PSMA-avid disease in this cohort was relatively low, as the inclusion criteria for study entry specifically required participants with either no evidence of disease, or only oligometastatic (<3 lesions) disease on bone scan and CT imaging. Additionally, the time between baseline and follow-up PSMA PET/CT imaging varied between 3 and 8 months. The variability in treatment effects and scan timing may limit the prognostic value of models fit in this study, and higher performance may be obtained if the analyses were repeated in a larger, prospectively gathered cohort.

## Conclusion

Patients with biochemically recurrent metastatic prostate cancer demonstrated heterogeneous response to treatment on  $^{68}\text{Ga}$ Ga-PSMA PET/CT, defined as the presence of new lesions or lesions increasing in PSMA uptake alongside disappearing lesions or lesions decreasing in PSMA uptake. Patients with heterogeneous response demonstrated significantly shorter OS than subjects with homogeneous response and homogeneous progression. Multiple PSMA imaging features were significantly associated with patient overall survival, with  $SUV_{total}$  at follow-up demonstrating the strongest association. When fitting multivariable models of survival, the inclusion of image features which capture lesion heterogeneity of change increased model performance. These results suggest that heterogeneous disease response on PSMA PET/CT imaging may have clinical significance in oligometastatic prostate cancer patients. When detected, there may be an opportunity to escalate treatment strategies to optimize patient outcomes.

### Clinical Practice Points

- Treatment of men with metastatic prostate cancer can be difficult due to the heterogeneity of response of lesions. [<sup>68</sup>Ga]Ga-PSMA-11 (PSMA) PET/CT assists with monitoring and directing clinical intervention; the response of individual lesions within a patient to treatment and its correlation with overall survival remains less explored. This study addresses this gap by analyzing PSMA PET/CT images from 162 men with metastatic prostate cancer over a 6 month period, using augmentative software to assess individual lesion response. The study reveals that 25% of men demonstrated heterogeneous responses, indicating different responses between lesions within the same patient. Importantly, this heterogeneous response pattern was associated with significantly shorter overall survival. The results also demonstrated that inclusion of lesion heterogeneity information improved the performance of multivariable outcome models. These findings underscore the importance of not only considering overall tumor response but also evaluating responses at the level of individual lesions. In clinical practice, identifying patients with heterogeneous responses early on could prompt closer monitoring and more timely clinical intervention. This personalized approach may lead to improved patient outcomes by enabling clinicians to tailor treatment strategies based on the distinct response patterns exhibited by individual lesions within a patient's tumor burden.

### Ethics Approval

This study was performed in line with the principles of the Declaration of Helsinki. Approval was granted by the Human Research Ethics Committees of Sir Charles Gairdner Hospital (RGS1736), Fiona Stanley Hospital (2015-125) and The University of Western Australia (2019/RA/4/20/6382).

### Data Availability

The datasets generated during and/or analyzed during the current study are not publicly available due to privacy and ethics restrictions. The data that support the findings of this study are available from the corresponding author upon reasonable request, but no personally identifying data can be provided.

### Consent to Participate

Informed consent was obtained from all individual participants included in the study.

### Consent to Publish

No individual participant data is included in the submitted manuscript.

### Disclosure

Financial interests: Author M.D. is supported by an AIQ Research Fellowship, a joint program established by AIQ Australia Pty. Ltd. and the University of Western Australia. Authors D.H., O.L., R.G., and T.P. are employees of AIQ Solutions. Nonfinancial interests: Author R.F. is a scientific advisory board member of AIQ Solutions.

### CRedit authorship contribution statement

**Mikaela Dell'Oro:** Writing – review & editing, Writing – original draft, Visualization, Validation, Supervision, Resources, Project administration, Methodology, Investigation, Formal analysis, Data curation, Conceptualization. **Daniel T. Huff:** Writing – review & editing, Writing – original draft, Methodology, Investigation, Formal analysis, Conceptualization. **Ojaswita Lokre:** Writing – review & editing, Software, Formal analysis, Conceptualization. **Jake Kendrick:** Writing – review & editing, Validation, Resources, Methodology, Data curation. **Rajkumar Munian Govindan:** Writing – review & editing, Validation, Software, Conceptualization. **Jeremy S.L. Ong:** Writing – review & editing, Resources, Methodology, Formal analysis, Data curation, Conceptualization. **Martin A. Ebert:** Writing – review & editing, Supervision, Resources, Project administration, Data curation, Conceptualization. **Timothy G. Perk:** Writing – review & editing, Supervision, Software, Funding acquisition, Conceptualization. **Roslyn J. Francis:** Writing – review & editing, Validation, Supervision, Project administration, Data curation, Conceptualization.

### Acknowledgments

This work was supported in part by the AIQ Research Fellowship, a joint program established by AIQ Australia Pty. Ltd. and the University of Western Australia. Research reported in this publication was supported by The National Cancer Institute of the National Institutes of Health under award number R44CA285006 and Royal Perth Hospital Imaging Research (4-3/0623). The content is solely the responsibility of the authors and does not necessarily represent the official views of the National Institutes of Health.

### References

1. Australian Institute of Health and Welfare. Cancer data in Australia [Internet]. Cancer data in Australia. 2023. Available from: <https://www.aihw.gov.au/reports/cancer/cancer-data-in-australia/contents/summary>. Accessed October 3, 2023.
2. Culp MB, Soerjomataram I, Efstathiou JA, Bray F, Jemal A. Recent global patterns in prostate cancer incidence and mortality rates. *Eur Urol*. 2020;77:38–52.
3. Paller CJ, Antonarakis ES. Management of biochemically recurrent prostate cancer after local therapy: evolving standards of care and new directions. *Clin Adv Hematol Oncol*. 2013;11:14–23.
4. Kyriakopoulos CE, Heath EI, Ferrari A, et al. Exploring spatial-temporal changes in 18 F-sodium fluoride PET/CT and circulating tumor cells in metastatic castration-resistant prostate cancer treated with enzalutamide. *J Clin Oncol*. 2020;38:3662–3671.
5. Ghosh A, Heston WDW. Tumor target prostate specific membrane antigen (PSMA) and its regulation in prostate cancer. *J Cell Biochem*. 2004;91:528–539.
6. Han S, Woo S, Kim YJ, Suh CH. Impact of 68Ga-PSMA PET on the management of patients with prostate cancer: a systematic review and meta-analysis. *Eur Urol*. 2018;74:179–190.
7. Maurer T, Eiber M, Schwaiger M, Gschwend JE. Current use of PSMA-PET in prostate cancer management. *Nat Rev Urol*. 2016;13:226–235.
8. Gafita A, Rauscher I, Weber M, et al. Novel framework for treatment response evaluation using PSMA PET/CT in patients with metastatic castration-resistant prostate cancer (RECIP 1.0): an international multicenter study. *J Nucl Med*. 2022;63:1651–1658.
9. Fanti S, Goffin K, Hadaschik BA, et al. Consensus statements on PSMA PET/CT response assessment criteria in prostate cancer. *Eur J Nucl Med Mol Imaging*. 2021;48:469–476.
10. Khreish F, Wiessner M, Rosar F, et al. Response assessment and prediction of progression-free survival by 68Ga-PSMA-11 PET/CT based on tumor-to-liver ratio (TLR) in patients with mCRPC undergoing 177Lu-PSMA-617 radioligand therapy. *Biomolecules*. 2021;11:1099.
11. Kurth J, Kretzschmar J, Aladwan H, et al. Evaluation of [68Ga]Ga-PSMA PET/CT for therapy response assessment of [177Lu]Lu-PSMA radioligand therapy in metastatic castration refractory prostate cancer and correlation with survival. *Nucl Med Commun*. 2021;42:1217–1226.

## Assessing the Heterogeneity of Response

12. Seitz AK, Rauscher I, Haller B, et al. Preliminary results on response assessment using 68Ga-HBED-CC-PSMA PET/CT in patients with metastatic prostate cancer undergoing docetaxel chemotherapy. *Eur J Nucl Med Mol Imaging*. 2018;45:602–612.
13. Harmon S, Perk T, Lin C, et al. MO-AB-BRA-05: [18F]NaF PET/CT imaging biomarkers in metastatic prostate cancer. *Med Phys*. 2016;43:3691.
14. Kendrick J, Francis RJ, Hassan GM, et al. Quantitative [68Ga]Ga-PSMA-11 PET biomarkers for the analysis of lesion-level progression in biochemically recurrent prostate cancer: a multicentre study. *Sci Rep*. 2023;13:17673.
15. McCarthy M, Francis R, Tang C, Watts J, Campbell A. A Multicenter prospective clinical trial of (68)Gallium PSMA HBED-CC PET-CT restaging in biochemically relapsed prostate carcinoma: Oligometastatic rate and distribution compared with standard imaging. *Int J Radiat Oncol Biol Phys*. 2019;104:801–808.
16. Wahl RL, Jacene H, Kasamon Y, Lodge M From RECIST to PERCIST: evolving considerations for PET response criteria in solid tumors. *J Nucl Med*. 2009;50(Suppl 1). Suppl 1122S-50S.
17. Kendrick J, Francis RJ, Hassan GM, et al. Ebert MAProspective inter- and intra-tracer repeatability analysis of radiomics features in [(68)Ga]Ga-PSMA-11 and [(18)F]F-PSMA-1007 PET scans in metastatic prostate cancer. *Br J Radiol*. 2023;96(1152):20221178.
18. Eisenhauer EA, Therasse P, Bogaerts J, et al. New response evaluation criteria in solid tumors: revised RECIST guideline (version 1.1). *Eur J Cancer*. 2009;45:228–247.
19. Joo Hyun O, Lodge MA, Wahl RL. Practical perclist: a simplified guide to PET response criteria in solid tumors 1.0. *Radiology*. 2016;280:576–584.
20. Box GEP, Cox DR. An analysis of transformations. *J R Stat Soc Series B Stat Methodol*. 1964;26:211–243.
21. lifelines, survival analysis in Python. 2021. Available from: <https://zenodo.org/records/8341606>. Accessed December 3, 2023.
22. R Core Team. R: a language and environment for statistical computing [internet]. Vienna, Austria: R Foundation for Statistical Computing; 2021. Accessed December 7, 2023. Available from: <https://www.R-project.org/>.
23. Gafita A, Djaileb L, Rauscher I, et al. Response evaluation criteria in PSMA PET/CT (RECIP 1.0) in metastatic castration-resistant prostate cancer. *Radiology*. 2023;308:e222148.
24. Harsini S, Wilson D, Sapruff H, et al. Outcome of patients with biochemical recurrence of prostate cancer after PSMA PET/CT-directed radiotherapy or surgery without systemic therapy. *Cancer Imaging*. 2023;23:27.
25. Hartrampf PE, Hüttmann T, Seitz AK, et al. SUVmean on baseline [18F]PSMA-1007 PET and clinical parameters are associated with survival in prostate cancer patients scheduled for [177Lu]Lu-PSMA 1&T. *Eur J Nucl Med Mol Imaging*. 2023;50:3465–3474.
26. Probst S, Bjartell A, Anand A, Skamene T, Ferrario C. Interval changes in PSMA PET/CT during radium-223 therapy for metastatic bone disease from castration-resistant prostate cancer. *Nucl Med Mol Imaging*. 2022;56:188–195.
27. Humbert O, Chardin D. Dissociated response in metastatic cancer: an atypical pattern brought into the spotlight with immunotherapy. *Front Oncol*. 2020;10:566297.
28. Dong Z, Zhai H, Hou Q, et al. Mixed responses to systemic therapy revealed potential genetic heterogeneity and poor survival in patients with non-small cell lung cancer. *Oncologist*. 2017;22:61–69.
29. Hendlisz A, Deleporte A, Delaunoy T, et al. The prognostic significance of metabolic response heterogeneity in metastatic colorectal cancer. *PLoS One*. 2015;10:e0138341.
30. Tazdait M, Mezquita L, Lahmar J, et al. Patterns of responses in metastatic NSCLC during PD-1 or PDL-1 inhibitor therapy: comparison of RECIST 1.1, irRECIST and iRECIST criteria. *Eur J Cancer*. 2018;88:38–47.
31. Tozuka T, Kitazono S, Sakamoto H, et al. Dissociated responses at initial computed tomography evaluation is a good prognostic factor in non-small cell lung cancer patients treated with anti-programmed cell death-1/ligand 1 inhibitors. *BMC Cancer*. 2020;20:207.
32. Kendrick J, Francis RJ, Hassan GM, Rowshanfarzad P, Ong JSL, Ebert MA. Fully automatic prognostic biomarker extraction from metastatic prostate lesion segmentations in whole-body [68Ga]Ga-PSMA-11 PET/CT images. *Eur J Nucl Med Mol Imaging*. 2022;50:67–79.
33. Zhao Y, Gafita A, Vollnberg B, et al. Deep neural network for automatic characterization of lesions on 68Ga-PSMA-11 PET/CT. *Eur J Nucl Med Mol Imaging*. 2020;47:603–613.
34. Trägårdh E, Enqvist O, Ulén J, et al. Freely available artificial intelligence for pelvic lymph node metastases in PSMA PET-CT that performs on par with nuclear medicine physicians. *Eur J Nucl Med Mol Imaging*. 2022;49:3412–3418.
35. Gafita A, Bieth M, Krönke M, et al. qPSMA: semiautomatic software for whole-body tumor burden assessment in prostate cancer using 68 Ga-PSMA11 PET/CT. *J Nucl Med*. 2019;60:1277–1283.